Korean J. Chem. Eng., **15**(3), 252-261 (1998)

SHEAR RATE DEPENDENCE OF THERMAL CONDUCTIVITY AND ITS EFFECT ON HEAT TRANSFER IN A NON-NEWTONIAN FLOW SYSTEM

Dong-Ryul Lee†

School of Automotive Engineering, College of Engineering, Catholic University of Taegu-Hyosung, 330, Keumrak 1-ri, Hayang-Eup, Kyungsan, Kyungbuk 712-702, Korea

(Received 12 August 1997 • accepted 12 March 1998)

Abstract – The purpose of this research was to investigate the extent to which the thermal conductivity of non-Newtonian fluids is affected by fluid motion, and then the effect of this shear-rate-dependent thermal conductivity, measured in Lee [1995], on the heat transfer for a typical convective system. Such information would have important implications in the design and analysis of non-Newtonian thermal systems such as are found in food processing operations, polymer processing, paint manufacturing, biological systems and many others. A simple parallel plate flow model with temperature-independent properties gave increases in heat transfer on the order of 30-80 % compared to the heat transfer with shear-rate-independent thermal conductivity in Newtonian fluid flow over the entire temperature range (20-50 °C) of CMC solutions depending on the inlet average velocity due to the effect of the shear-rate-dependent thermal conductivity.

Key words: Non-Newtonian Fluid Flow, Thermophysical Property, Parallel Duct, Thermal Conductivity, Non-Newtonian Heat Transfer Coefficient

INTRODUCTION

Non-Newtonian or rheological fluids are used in many practical applications. This can be illustrated by listing a number of such fluids. Some examples: paints, pharmaceuticals, inks, food products, suspensions, blood and other body fluids, polymer solutions, coal-water mixtures, etc. Most of these belong to the class of purely viscous non-Newtonian fluids that are defined as those fluids in which the shear stress in the fluid is a function only of the shear rate (or velocity gradient). For non-Newtonian fluids, this functional relationship is non-linear. Those fluids that have a linear relationship between the shear stress and shear rate are defined as Newtonian fluids.

There has been a renewed interest in recent years in obtaining more quantitative information about non-Newtonian fluids in order to better understand their physical nature and to optimize their use in practical applications. Many studies have been carried out to investigate their viscous properties, i.e., the above-mentioned relation between the shear stress and shear rate. Such information is required in order to be able to solve the basic equations of fluid motion.

Most of the investigations mentioned above, however, have dealt with isothermal systems. When temperature differences exist within a system, it is necessary to solve the equations of fluids along with the fluid energy equation in order to determine the internal or boundary heat transfer. In this case, a knowledge of the thermal properties is required, and, in particular, the thermal conductivity of the fluid must be known.

†To whom all correspondence should be addressed.
E-mail: dlee@cuth.cataegu.ac.kr

Although the viscous properties of non-Newtonian fluids have been, and continue to be, thoroughly investigated, this is not the case for the fluid thermal conductivities. A few investigations have been reported for polymer mixtures which have indicated that for low polymer concentrations, less than 1 % by weight, the thermal conductivity of the solution is the same as the solvent. At larger concentrations, the thermal conductivity appears to increase slightly.

The most interesting aspect of the previous investigations, however, is that all of the measurements have been made under static conditions, i.e., the fluid was stationary when the thermal conductivities were measured. If there are significant non-Newtonian effects on the thermal conductivity, then the measurements must be made over an appropriate shear rate range when the fluid is moving with respect to a stationary boundary.

A few investigations have been made to study the influence of shear rate on the thermal conductivity of polymer solutions, but the results have been confusing and contradictory. Cocci and Picot [1973] and Chitrangad and Picot [1981] observed that at low shear rates the thermal conductivity increased with shear rate, reached a maximum and then decreased with shear rate. The thermal conductivity change from the minimum to the maximum was on the order of 20 %.

Conversely, Wallace et al. [1985] found that depending on the polymer molecular weight, there was either an increase of thermal conductivity with shear rate and a leveling off, or a decrease in thermal conductivity with shear rate and a leveling off. Thermal conductivity changes with shear rate up to 55 % were reported.

When investigating the influence of convective heat trans-

fer on typical thermal systems, one generally assumes that the thermophysical properties of fluids are constant. However, such an assumption could result in significant errors in the case where it is applied to the actual heat transfer systems. This research concerns the experimental determination of the thermal conductivity of non-Newtonian fluids under conditions when the liquid is in motion and the measured values of the thermal conductivity are used to calculate heat flows under a variety of conditions. In this research, a simple convection heat transfer problem is considered to compare the change in heat flow for a non-Newtonian fluid if the thermal conductivity is taken as a function of shear rate as determined by the present experiments. This heat flow is then compared with the heat flow when the thermal conductivity is considered to be independent of shear rate.

Central to the problem of duct design is the prediction of pressure drop and heat transfer in the duct passages. In order to make such predictions for non-Newtonian fluids, it is necessary to know the relation between the viscous and thermal properties of the fluid and the wall shear rate. This is done by assuming constitutive equations which relate the local apparent viscosity and thermal conductivity of the fluid to the local shear rate. The power-law equation is an often used constitutive equation of viscosity; the constitutive equation of thermal conductivity will be developed and discussed later in the analysis section.

An understanding of fully developed laminar flow in ducts can be acquired by investigating a simple flow situation. It was discussed previously that the viscous and thermal properties are a rather strong function of temperature for many power-law fluids. Therefore, special caution should be made in using constant property solutions for actual design calculations. Nonetheless, the concept of fully developed flow is a useful one for conceptual purposes and for isolating the significant physical processes in a duct flow system.

Previous works of heat transfer analysis regarding heat exchanger duct flows with shear-rate-dependent thermal conductivity have not been found to date in the literature. No direct comparison can be made with literature values because no reported values of such solutions are available.

The purpose of this study was to measure the viscous properties of a non-Newtonian fluid such as a CMC solution, a purely viscous fluid. Also, to be measured were the thermal conductivities of the same fluid under dynamic conditions over a shear rate range, where the viscous properties change significantly with shear rate, in order to examine any effect of the thermal conductivity in a shear field on the heat transfer of a typical convective thermal system. If significant shear rate dependencies for the thermal conductivities are observed, this would have important implications in the analyses of non-Newtonian thermal systems.

VISCOUS PROPERTY MEASUREMENTS

1. Description of Pseudoplastic Fluids

By examining the viscous properties of non-Newtonian fluids, one can obtain some knowledge about the proposed measurement technique for thermal conductivities. Fig. 1 is a sketch of a flow curve of a typical pseudoplastic fluid. The ordinate is the logarithm of the apparent viscosity which is the ratio of the shear stress to the shear rate and the abscissa is the logarithm of the shear rate. For Newtonian fluids, $\tau = \eta_a \dot{\gamma}$ is the constitutive equation with the dynamic viscosity, η_a, as the fluid property. Referring to Fig. 1, at low shear rates the fluid exhibits a Newtonian viscosity which is independent of the flow field or the shear rate and is a horizontal line on the flow curve. However, the apparent viscosity curve decreases in the transition region and becomes log linear in the power-law region at higher shear rates. Fig. 1 is indicative of the behavior of many purely viscous pseudoplastic fluids. According to the curve in Fig. 1 it is seen that at lower shear rates (region I) the fluid is Newtonian ($\eta_a=\eta_0$=constant). The viscosity at zero shear rate is called the zero shear rate viscosity. At higher shear rates (region II), the apparent viscosity starts to decrease until it turns into a straight line (region III). In the lower shear rate range, the fluid is Newtonian ($\eta_a=\eta_0$) and in the higher shear rate range the fluid behaves as a power-law fluid ($\eta_a=K\dot{\gamma}^{n-1}$).

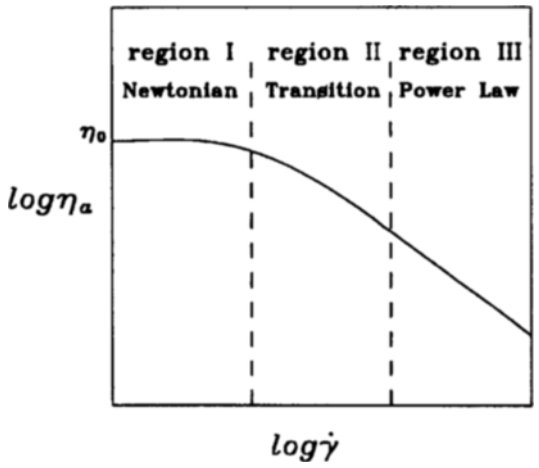

Fig. 1. Typical flow curve for a pseudoplastic fluid.

The purpose of this investigation was to measure the thermal conductivity of non-Newtonian fluids in the power-law region to determine if this thermal property is a function of shear rate as is another transport property, the dynamic viscosity.

2. Method of Viscous Property Measurements

The falling needle viscometer (FNV) was used to measure the apparent viscosities of non-Newtonian fluids. The FNV consists of a slim hollow needle with hemispherical ends inserted into the needle launcher and falling through the test fluid under the influence of gravity in a cylindrical container. The longitudinal axes of the needle and the container are parallel to the gravitational direction. After the needle velocity reaches a constant or terminal value, the needle velocity in the container may be determined either by locating the small magnet in the downward needle tip and using Hall sensors on the measurement lines for opaque fluids or by visually measuring the elapsed time, with a stop watch, for the needle to travel between two lines drawn on the outside of the container. Therefore, the only experimental measurements which are performed to determine any of the rheological properties of the

experimental fluids are the temperature of the system and an elapsed time [Park and Irvine, 1988]. These measurements can then be converted into the final rheological properties such as the flow index, fluid consistency, zero shear rate viscosity, and apparent viscosity by the appropriate methods as described in Park and Irvine [1988] and Park [1984].

To determine flow curves, a graph must be plotted of $\ln(\rho_s - \rho_l)$ on the ordinate and $\ln U_t$ on the abscissa. U_t denotes the measured terminal velocity of the falling needle, and ρ_s and ρ_l denote the density of the falling needle and density of the fluid, respectively. If the fluid is a Newtonian or power-law fluid over the operating shear rate range of the needle runs, the data will form a straight line. The slope of this line will be the value of the flow index, n and the ordinate intercept at $\ln U_t$ will yield the flow consistency, K.

The measurements exhibited in Fig. 2 were conducted by Lee [1995] with a falling needle viscometer by following the procedures of Park and Irvine [1988]. Fig. 2 indicates the curves of apparent viscosity plotted against shear rate for the CMC solutions measured in Lee [1995] and also shows that if $\dot{\gamma}>100$ (1/s), the apparent viscosity is in the power-law range. A careful investigation of Fig. 2 shows that the power-law equation is only applicable at high shear rates where the straight line portion of the curve exists. The rheological properties of the CMC solutions, using the power-law model as mentioned above, are presented in Table 1. Having determined the power-law region for the polymer solutions (CMC 1500, 2500, and 5000 wppm), we then assembled an experiment to measure the thermal conductivities in these shear rate regions.

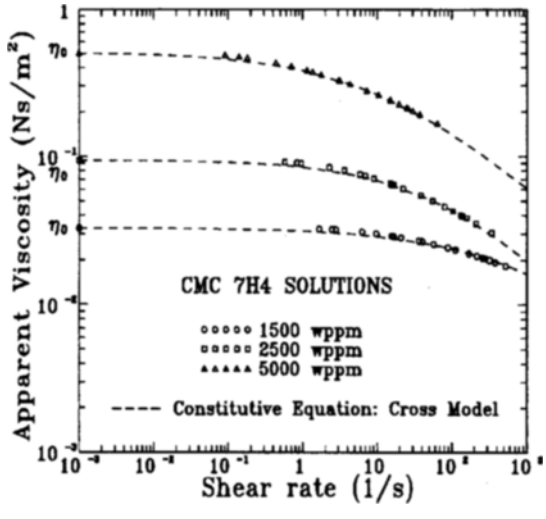

Fig. 2. Apparent viscosity of CMC solutions (1500, 2500, and 5000 wppm) plotted against shear rate.

Table 1. Rheological properties for power-law model

Solutions (wppm)	η_0 (Ns/m^2)	Power-law model	
		n	K (Ns/m^2)
CMC 1500	0.0329	0.8350	0.0522
CMC 2500	0.0949	0.6941	0.1839
CMC 5000	0.5116	0.6733	0.6787

EXPERIMENTAL DEVICE FOR THERMAL CONDUCTIVITY MEASUREMENTS

1. General Description of Experimental Apparatus and Design Considerations

Thermal conductivities in a shear field were measured over approximately the same power-law shear rate range as in Fig. 2 where the viscous properties show strong non-Newtonian effects. For the purpose of performing this, an experimental set-up such as in Fig. 3 was utilized.

Fig. 3 shows a schematic of a coaxial cylinder system where the inner cylinder is quiescent and the outer cylinder is rotating. The experimental fluid is located in the annular gap, which is 1.25 mm. Thus a Couette type flow is built up between the cylinders if the gap width is small enough compared to the radius of the inner cylinder. The inner cylinder consists of a thermal probe containing a heating coil. The dual cylinder assembly was located in a constant temperature bath to keep the outer cylinder at a known and constant temperature. The temperature difference across the gap was about 10 °C.

The apparatus for the measurements of non-Newtonian thermal conductivities in a shear field is shown in Fig. 4. This system consists of a constant temperature bath, a rotating outer cylinder, stationary inner cylinder, digital multimeter, power supply, rotating mechanism and calibrated thermocouples, T_1 and T_2, to measure the inner cylinder temperature. The required measurements are the wall temperature difference between the inner and the outer cylinder ($\triangle T$), heat flow rate (Q), length of the cylinder (l), ratio of the outer cylinder to the inner cylinder radius (r_o/r_i), wire resistance (R_T), wire voltage (E), wire current (I), and angular velocity of the outer cyl-

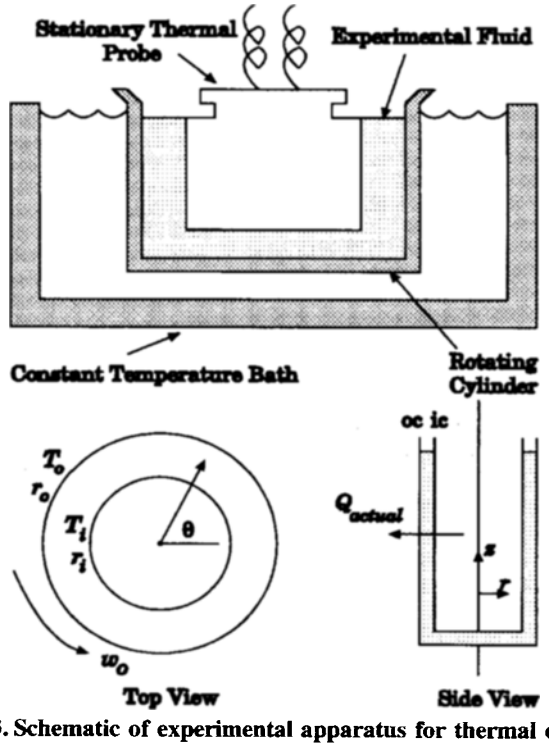

Fig. 3. Schematic of experimental apparatus for thermal conductivity measurements in a shear field.

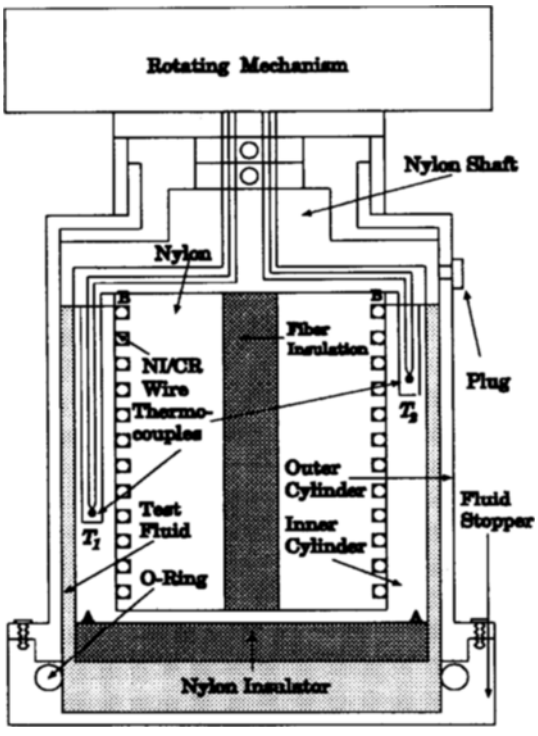

Fig. 4. Schematic of the thermal conductivity cell.

inder (w_o).

Possible uncertainty in the shear rate measurements could be caused by the fact that the apparent viscosity of the fluid changes across the gap due to the temperature gradient from the inner to the outer cylinder. This would cause the shear rate to decrease from the inner to the outer cylinder, which is opposite in effect to the shear rate change caused by curvature. This thermal shear rate change is the same order of the magnitude as the curvature change and therefore would tend to reduce the overall shear rate uncertainty. This cancellation of errors was not applied, however, and the shear rate presented and considered in the error analysis is the average between the cylinder considering only the curvature effect.

During an experimental run, the measurements includes the rotational velocity of the outer cylinder, the temperature difference between the inner and the outer cylinder, and the heat input from the power supply [Lee, 1995].

2. Derivation of Working Equations

Many viscous liquids exhibit a significant amount of viscous dissipation that causes an increase in fluid temperatures, thereby affecting the heat transfer rate at the wall. Normally the Brinkman number is used as a measure of viscous dissipation and the extent to which viscous heating is important relative to the heat flow resulting from the temperature difference ($T_{inner} - T_{outer}$). In general, a Brinkman number on the order of 1 indicates significant viscous dissipation.

The effect of viscous heating in both Newtonian and non-Newtonian fluids could have a significant effect in the coaxial rotating cylinder system used in the present experiment. Thus it must be determined that the Brinkman number is much less than unity. Brinkman numbers have been calculated over the operating region of the present experiment, and the maximum power-law Brinkman number was 0.024. Thus no obvious viscous dissipation effects are to be expected in the operating power-law region.

If free convection could occur between the two vertical cylinders, the thermal conductivity measurements would be in error. As reported by Eckert and Drake [1972], there is a critical Rayleigh number of 1000 below which heat transfer between the two cylinders takes place only by pure conduction. In the present experiment, the maximum Rayleigh number occurs for the lowest viscosity fluid, i.e., water. In this water case, the maximum Rayleigh number was 261 and therefore no free convection effects are to be expected. That this was the case will be illustrated when the water thermal conductivity measurements are presented below.

In order to specify an energy equation for a flowing fluid, it is necessary to have a law which describes the heat conduction in the fluid. If Fourier's law of heat conduction is used, i.e.,

$$q = -k\frac{dT}{dr} \tag{1}$$

The question to be addressed is whether in Eq. (1) k is a function of shear rate. Assume the temperature-independent thermal conductivity of the non-Newtonian fluid is a function of shear rate only ($k(\dot{\gamma})$) if there is no viscous dissipation. Using Fourier's law, the heat flow rate will be described with the following equation

$$Q = -k(\dot{\gamma})2\pi rl\frac{dT}{dr} \tag{2}$$

where $\dot{\gamma} = r\frac{d}{dr}\left(\frac{u_\theta}{r}\right)$. Integration of Eq. (2) can be written as follows;

$$\int_{r_i}^{r_o}\frac{dr}{rk(\dot{\gamma})} = -\int_{T_i}^{T_o}\frac{2\pi l}{Q}dT$$

$$\int_{r_i}^{r_o}\frac{dr}{rk(\dot{\gamma})} = \frac{2\pi l}{Q}(T_i - T_o) \tag{3}$$

where the uncertainty of the temperature difference effect (10 °C) on the thermal conductivity is about 2 %, whose value results in the measurement error compared to the standard literature value of water.

Since the shear rate in the cylindrical gap is essentially constant in Couette flow, $k(\dot{\gamma})$ can be taken out from the integral in Eq. (3) giving

$$k = \frac{\int_{r_i}^{r_o}\frac{dr}{r}}{\frac{2\pi l}{Q}(T_i - T_o)}$$

$$k = \frac{Q\ln\frac{r_o}{r_i}}{2\pi l(T_i - T_o)} \tag{4}$$

Eq. (4) is the working equation for the present apparatus. The remainder of this section will deal with the correctness of this working equation.

3. Stability of the Non-Newtonian Fluid Flow

It is well known that under certain circumstances secondary flows can occur in rotating Couette flows [Taylor, 1923].

These flows would increase the measured thermal conductivities; therefore an investigation was carried out as to the possibility of their occurrence. At Taylor numbers above a critical value based on angular velocity of the rotating cylinder, the average gap radius, and the cylinder gap, a secondary flow between two concentric cylinders can occur depending upon which cylinder is rotating. However, when the inner cylinder is at rest and the outer one is rotating, the motion in a viscous Newtonian fluid under these circumstances was shown to be always stable even with very high speeds of the outer cylinder.

The present range of the Taylor numbers over the three concentrations used (CMC 1500, 2500, and 5000 wppm) was less than the critical Taylor numbers from the data of gap width, flow index, fluid density, and fluid consistency as described in Sinevic et al. [1986] for CMC solutions and Larson [1989] for Separan solutions. Therefore, the flow of the fluids in the present experiments is believed to be stable even though the Ta_{cr} number is for a rotating inner cylinder. A further confirmation of the flow stability can be found in the work of Park et al. [1990]. In this study the apparent viscosity vs. shear rate was measured for a 2000 wppm water solution of Separan. For a rotating cylinder viscometer and falling needle viscometer, the data from the two instruments showed excellent agreement even though the falling needle viscometer is a non-rotating system. In addition, the temperature gradient direction with respect to the centrifugal force is such as to result in a stable thermal system [Lee, 1995].

EXPERIMENTAL RESULTS FOR NEWTONIAN AND NON-NEWTONIAN FLUIDS

A series of measurements were made on distilled water to calibrate the apparatus before the thermal conductivity measurements of the non-Newtonian fluids were conducted. The objective of these measurements was to determine that the apparatus could measure the well documented values of water thermal conductivity and to verify that there were no obvious shear rate effects on the water data since water is a Newtonian fluid, and that no appreciable free convection effects were present.

Fig. 5 reveals the results of the water measurements. Three things are apparent in the figure. First, the water thermal conductivity data agree within 2% of the reported values of Haar et al. [1984] at shear rates greater than approximately 100 s^{-1} and thus no free convection effects are apparent. Second, there is no definite shear rate effect over the shear rate range of interest. Third, at low shear rates the thermal conductivity values are low. An investigation of this latter effect indicated that the reason was a low heat transfer coefficient at the outer cylinder at low rotational speeds. This caused the outer cylinder temperature to be higher than the bath temperature. Attaching several longitudinal convecting fins to the outer cylinder to increase the convective heat transfer coefficient solved this problem. This resulted in moving the low thermal conductivity data outside the range of the operating shear rate (60 to 900 s^{-1}).

Figs. 6-9 show the curves of thermal conductivity vs. shear rate for CMC 7H4 5000, 2500, and 1500 wppm solutions at

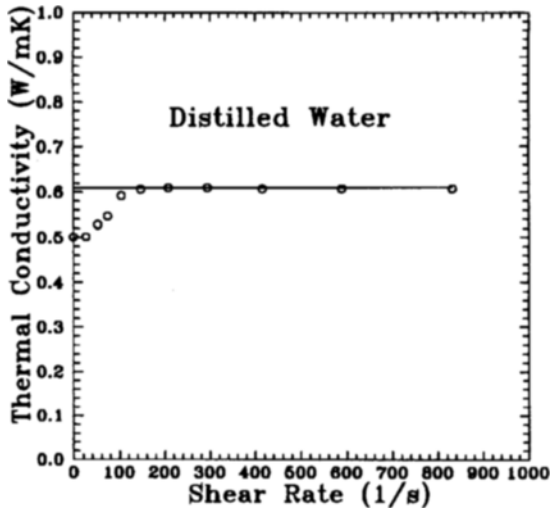

Fig. 5. Thermal conductivity vs. shear rate for distilled water at fluid temperature (26 °C) without convecting fins, — Haar et al. [1984] ○ – present data.

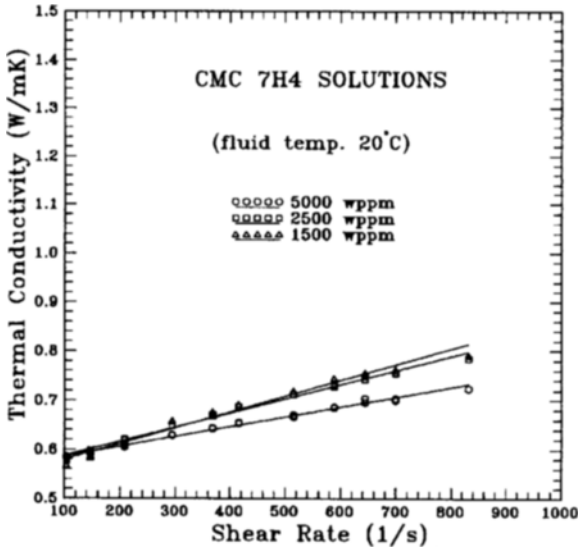

Fig. 6. Thermal conductivity vs. shear rate for CMC solutions (5000, 2500, and 1500 wppm) at 20 °C.

temperatures 20, 30, 40 and 50 °C, respectively. The thermal conductivity increased significantly with shear rate on a fixed temperature unlike the tendency of non-Newtonian viscosity with shear rate. Figs. 6-9 and Table 2 exhibit an obvious dependence of thermal conductivity on shear rate as similarly reported in Loulou [1992] and Chaliche et al. [1994]. As shown in Figs. 6-9, the solid lines are least square curve-fits at various temperatures, which show good agreements with the actual experiment data within 2% differences.

No direct comparisons can be made with literature values because no reported values of such solutions are available. Higher concentration solutions of CMC in the range of 30000 -80000 wppm) are available only over a low shear rate range ($0 \leq \dot{\gamma} \leq 60$ s^{-1}) in Chaliche et al. [1994]. Regarding the general trends of the curves in a shear field, both the present measurements and theirs show increasing thermal conductivities

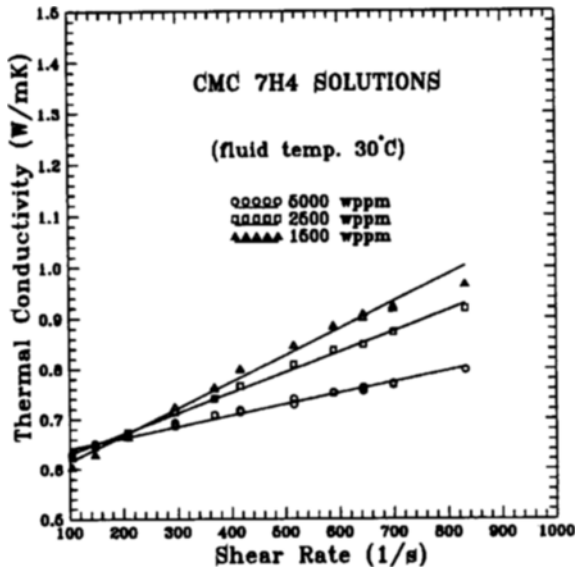

Fig. 7. Thermal conductivity vs. shear rate for CMC solutions (5000, 2500, and 1500 wppm) at 30 °C.

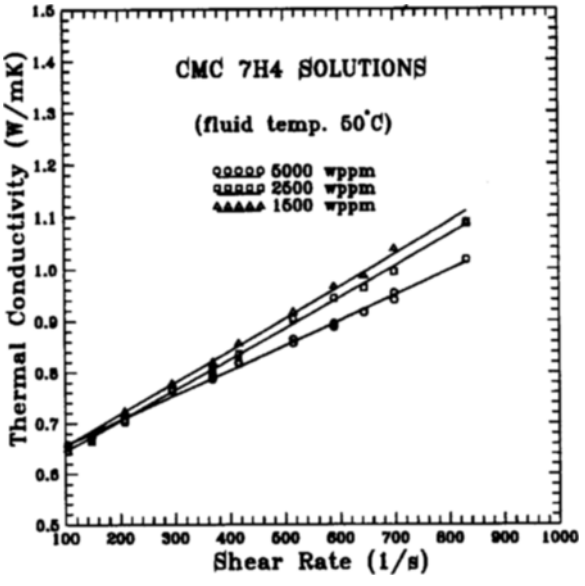

Fig. 8. Thermal conductivity vs. shear rate for CMC solutions (5000, 2500, and 1500 wppm) at 40 °C.

with shear rate.

Table 2 shows the change of thermal conductivity over the entire operating shear rate region ($100 \leq \dot{\gamma} \leq 900$ s $^{-1}$). Similar to Newtonian fluids, the thermal conductivity of non-Newtonian purely viscous fluids increases with temperature.

ANALYSIS OF HEAT TRANSFER WITH SHEAR-RATE-DEPENDENT THERMAL CONDUCTIVITY

A reasonable way of expressing the shear-rate-dependent thermal conductivity and which represents the present experimental data is

$$k = k_0 + (\dot{\gamma} - \dot{\gamma}_0) \tan\alpha \quad (5)$$

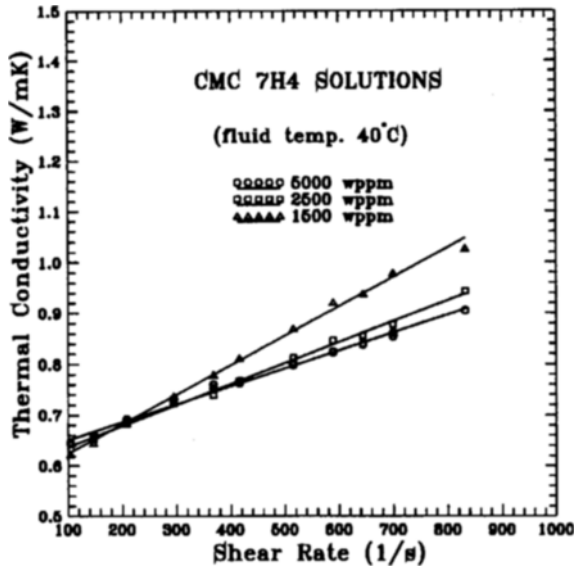

Fig. 9. Thermal conductivity vs. shear rate for CMC solutions (5000, 2500, and 1500 wppm) at 50 °C.

Table 2. Inclination angle of shear rate on shear-rate-dependent thermal conductivity

Solutions	α (°)	Temperature (°C)	$\dot{\gamma}_{min}$ (W/mk)
CMC 7H4	0.0109	20	0.586
5000 wppm	0.0139	30	0.629
	0.0207	40	0.648
	0.0281	50	0.657
CMC 7H4	0.0162	20	0.578
2500 wppm	0.0232	30	0.621
	0.0237	40	0.642
	0.0332	50	0.663
CMC 7H4	0.0177	20	0.569
1500 wppm	0.0287	30	0.605
	0.0317	40	0.624
	0.0345	50	0.652

where k_0 is zero shear rate thermal conductivity, $\dot{\gamma}_0$ is the minimum operating shear rate, and α is the inclination angle of shear rate on shear-rate-dependent thermal conductivity. The present linear data reduction of non-Newtonian fluids can be compared with the present experimental data in Figs. 6-9. This gives a good agreement with the experimental data with a ± 2 % difference.

An understanding of fully developed laminar flow in ducts can be acquired by investigating a simple flow situation. It was discussed previously that the viscous and thermal properties are a rather strong function of temperature for many power-law fluids. Therefore, special caution should be taken in using constant property solutions for actual design calculations. Nonetheless, the concept of fully developed flow is a useful one for conceptual purposes and for isolating the significant physical processes in a duct flow system.

Consider the flow through two infinite stationary parallel plates which are a distance 2a apart with steady fluid flow through the duct. If a shear-rate-variable thermal conductivity

which is temperature-independent is applied to fully developed parallel flat plate flow with a view to further understanding the shear rate effect of thermal conductivity on heat transfer, the governing equation on a fluid element, dx − dy, can be written as follows, where x is the flow direction and y is normal to flow direction in the parallel plates

$$\frac{\partial}{\partial y}\left(\eta_a \frac{\partial u}{\partial y}\right) = -\frac{dp}{dx} \tag{6}$$

$$\frac{\partial}{\partial y}\left(k\frac{\partial T}{\partial y}\right) = \rho C_p u \frac{dT_B}{dx} \tag{7}$$

where

$$q_w = \rho C_p \bar{u} a \frac{dT_B}{dx}$$

and C_p is specific heat, $\bar{u}$ is the average velocity in flow direction, and T_B is the bulk temperature. The boundary conditions for the above governing equations are

$$y = 0, \qquad \frac{\partial u}{\partial y} = 0$$

$$y = a, \qquad u = 0$$

where a is the half width of the parallel duct.

Making the parameters and variables dimensionless, it will be described with the following:

$$y^+ = \frac{y}{a}, \qquad u^+ = \frac{u}{\bar{u}}$$

$$T^+ = \frac{T - T_w}{T_B - T_w}, \qquad T^{++} = \frac{T^+}{Nu}$$

$$k^+ = \frac{k}{k_0}, \qquad Re_g = \frac{\rho \bar{u}^{2-n} a^n}{K}$$

$$Nu = \frac{ha}{k_o}, \qquad \frac{dp}{dx} = \frac{\rho \bar{u}^2 f}{2a} \tag{8}$$

where

$$Nu = \frac{ha}{k_0} = \frac{1}{\int_0^1 u^+ T^{++} dy^+}$$

$$Nu_0 = \frac{h_0 a}{k_0} = \frac{\left[\frac{1}{4}\int_0^1 [\int_0^{y^+} u^+ dy^+]^2 dy^+\right]^{-1}}{4}$$

and T_w is the wall temperature of the parallel plate, K is the flow index of the power-law fluid, and Re_g is the generalized Reynolds number ($\rho \bar{u}^{2-n} a^n/K$) for the power-law fluid, and Nu is average Nusselt number for a duct at varying shear rate and Nu_0 is average Nusselt number for a duct with shear rate independent thermal conductivity referenced from Bird et al. [1977].

The dimensionless energy equation for the power-law fluid can be written by a new formation using Eq. (5)

$$k^+ = 1 + \frac{(\dot{\gamma} - \dot{\gamma}_0)}{k_0} \tan\alpha \tag{9}$$

If $\dot{\gamma}$ is equal to $\dot{\gamma}_0$, then k^+ becomes 1. Letting $\dot{\gamma}^+ = \frac{\dot{\gamma}\tan\alpha}{k_0}$, then the dimensionless thermal conductivity should be written as follows;

$$k^+ = 1 + (\dot{\gamma}^+ - \dot{\gamma}_0^+) \tag{10}$$

By deriving from the momentum Eq. (6) using the dimensionless parameter fRe_g from the relation between $\bar{u}$ and $\frac{dp}{dx}$ $\left(f = \frac{2\frac{dp}{dx}a}{\rho \bar{u}^2}\right)$ with power law, the dimensionless velocity gradient can be derived as

$$\frac{du^+}{dy^+} = \left(\frac{fRe_g}{2}\right)^{\frac{1}{n}} y^{+\frac{1}{n}} \tag{11}$$

$$u^+ = \left(\frac{fRe_g}{2}\right)^{\frac{1}{n}} y^{+\frac{1}{n}} \frac{n}{n+1}\left(1 - y^{+\frac{n+1}{n}}\right) \tag{12}$$

$$\dot{\gamma}_0^+ = \frac{\dot{\gamma}_0 a}{\bar{u}} \tag{13}$$

$$\dot{\gamma} = \frac{\bar{u}}{a}\left(\frac{fRe_g}{2}\right)^{\frac{1}{n}} y^{+\frac{1}{n}} \tag{14}$$

with additional definitions,

$$\bar{u}^+ = \frac{\bar{u}\tan\alpha}{k_0 a} \tag{15}$$

$$\dot{\gamma}^+ = \frac{\bar{u}\tan\alpha}{k_0 a}\left(\frac{fRe_g}{2}\right)^{\frac{1}{n}} y^{+\frac{1}{n}} = \bar{u}^+\left(\frac{fRe_g}{2}\right)^{\frac{1}{n}} y^{+\frac{1}{n}} \tag{16}$$

$$\dot{\gamma}_0^+ = \frac{\bar{u}\tan\alpha}{k_0 a}\left(\frac{fRe_g}{2}\right)^{\frac{1}{n}} y^{+\frac{1}{n}} = \bar{u}_0^+\left(\frac{fRe_g}{2}\right)^{\frac{1}{n}} y^{+\frac{1}{n}} \tag{17}$$

$$\dot{\gamma}^+ - \dot{\gamma}_0^+ = (\bar{u}^+ - \bar{u}_0^+)\left(\frac{fRe_g}{2}\right)^{\frac{1}{n}} y^{+\frac{1}{n}} \tag{18}$$

where the magnitude of fRe_g is cited from Irvine and Karni [1987], $\bar{u}^+$ is the dimensionless average velocity at the varying average velocity, and $\bar{u}_0^+$ is the dimensionless average velocity at the minimum average velocity when $\bar{u}=\bar{u}_0$. If $\bar{u}^+ = \bar{u}_0^+$, then $\dot{\gamma}^+ - \dot{\gamma}_0^+ = 0$ and $k^+ = 1$. The energy Eq. (7) becomes

$$\frac{d}{dy^+}\left[\{1 + (\dot{\gamma}^+ - \dot{\gamma}_0^+)\}\frac{dT^+}{dy^+}\right] = u^+ Nu \tag{19}$$

$$\frac{d}{dy^+}\left[\left\{1 + (\bar{u}^+ - \bar{u}_0^+)\left(\frac{fRe_g}{2}\right)^{\frac{1}{n}} y^{+\frac{1}{n}}\right\}\frac{dT^+}{dy^+}\right] = u^+ Nu \tag{20}$$

This means that $(\bar{u}^+ - \bar{u}_0^+)\left(\frac{fRe_g}{2}\right)^{\frac{1}{n}} = \triangle\bar{u}^+\left(\frac{fRe_g}{2}\right)^{\frac{1}{n}}$ is the parameter and if $\triangle\bar{u}^+ = 0$, there is no dependence of k on $\dot{\gamma}$.

For a power-law fluid, the differential equation becomes

$$\frac{d}{dy^+}\left[\left\{1+\triangle\bar{u}^+\left(\frac{fRe_g}{2}\right)^{\frac{1}{n}}y^{+\frac{1}{n}}\right\}\frac{dT^{+}}{dy^+}\right]=u^+ \qquad (21)$$

Boundary conditions are:

$$T^+=0, \qquad y^+=1$$
$$\frac{\partial T^+}{\partial y^+}=0, \qquad y^+=0 \qquad (22)$$

From the above equations, the velocity, temperature distributions, and the heat transfer with non-Newtonian properties can be obtained by numerical analysis. The results are shown in the following groups of figures and tables.

RESULTS AND DISCUSSION

Table 2 indicates that for CMC solutions the inclination angle of the shear rate (α) to the shear-rate-dependent thermal conductivity is a strong function of temperature. As seen in Table 2, the lower solution concentration has a larger angle (α) than the higher concentration at a certain temperature, which illustrates once again that the increase of thermal conductivity with operating shear rate is higher for the lower concentration solution than that for the higher concentration. Table 2 does not always show the shear rate dependence up to the zero concentration limit, but a possible optimal concentration level. The fact that the shear rate dependence is stronger in the lower concentration is no longer valid in the region where the optimal concentration level does not exist. It also shows that the angle increases as the thermal conductivity at the minimum operating shear rate increases at certain concentrations. For structured liquids such as non-Newtonian fluids, imposition of a shear field alters the structural state of the liquid and hence its thermal conductivity. As a result, thermal conductivity becomes shear-rate-dependent. As shear rate increases, the molecular entanglements start to play a dominant role. The rise in the thermal conductivity at higher shear rates is attributable to the formation of rotating units of entangled clusters. The increase in thermal conductivity with shear rates is suggestive of a different flow mechanism. High polymer liquids will undergo a change in the mechanism of flow when the elastic energy stored in the random coils becomes of the same order of magnitude as the amount of viscous heat generated at the entanglement junctions.

Figs. 10-13 present the data of the dimensionless heat transfer coefficient vs. the dimensionless parameter $\left\{\triangle\bar{u}^+\left(\frac{fRe_g}{2}\right)^{\frac{1}{n}}\right\}$ in the fully developed parallel flat plates for three solutions of CMC at temperatures (20, 30, 40, and 50 °C). These figures also indicate that the heat transfer coefficient increases with average velocity difference for a given fluid with a sim-

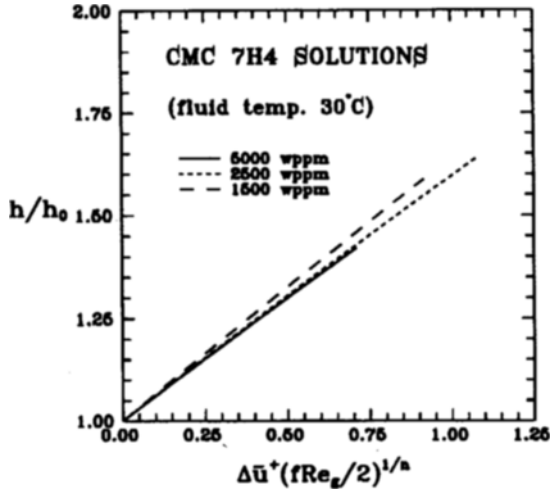

Fig. 11. Dimensionless heat transfer coefficient vs. dimensionless average velocity difference in the fully developed parallel plates for CMC solutions (5000, 2500, and 1500 wppm) at 30 °C.

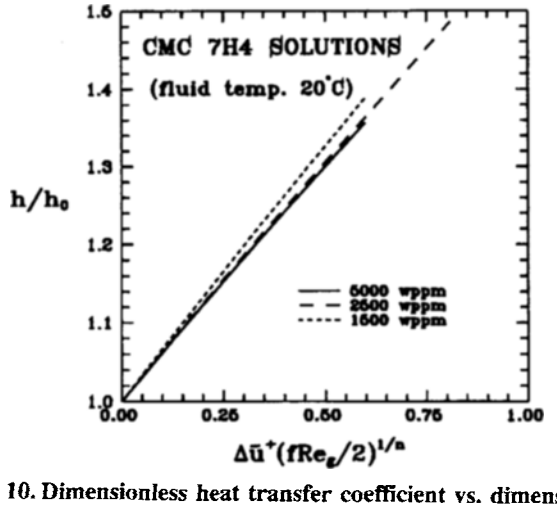

Fig. 10. Dimensionless heat transfer coefficient vs. dimensionless average velocity difference in the fully developed parallel plates for CMC solutions (5000, 2500, and 1500 wppm) at 20 °C.

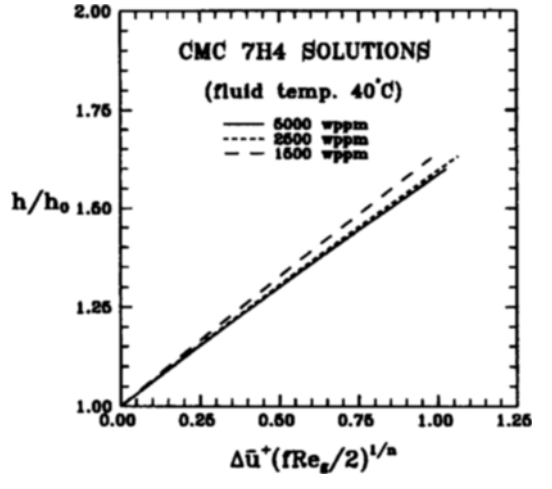

Fig. 12. Dimensionless heat transfer coefficient vs. dimensionless average velocity difference in the fully developed parallel plates for CMC solutions (5000, 2500, and 1500 wppm) at 40 °C.

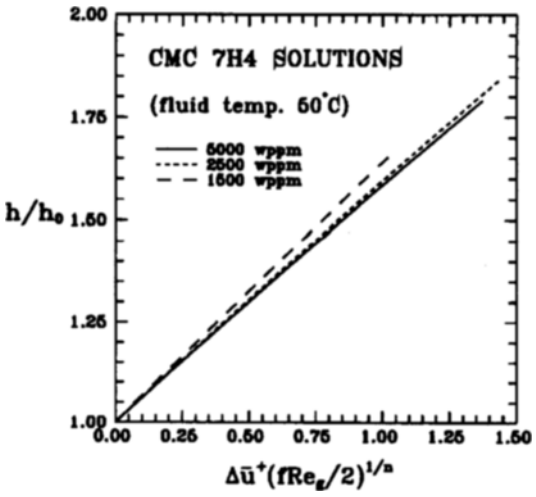

Fig. 13. Dimensionless heat transfer coefficient vs. dimensionless average velocity difference in the fully developed parallel plates for CMC solutions (5000, 2500, and

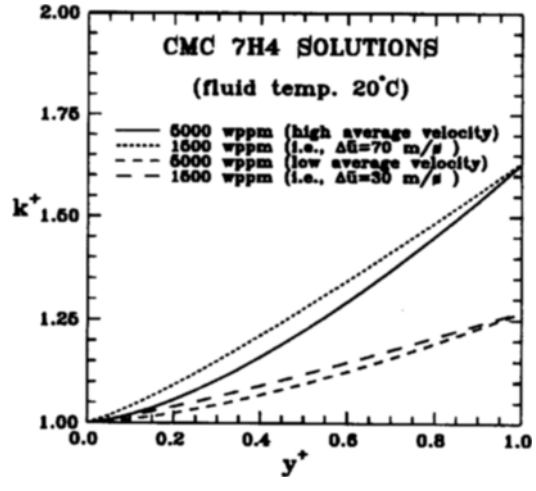

Fig. 14. Dimensionless thermal conductivity vs. dimensionless duct cross-section locations for CMC solutions (5000 and 1500 wppm) with the maximum and half of the maximum average velocities.

ilar degrees of increase on the heat transfer in the similar manner to the Couette flow curves of thermal conductivity against shear rate as shown in Figs. 6-9 with solid lines. It is also seen that a low concentration solution transfers more heat than a higher concentration solution with the same average velocity according to Figs. 10-13.

Fig. 14 shows curves of the shear-rate-dependent thermal conductivity at various duct cross-section locations for different concentrations of CMC solutions with two different average velocities, respectively. Thus:

- The thermal conductivity with a large average velocity is larger than that with a low average velocity at any location in the cross-section.
- The thermal conductivity with a higher concentration is smaller than that with a lower concentration at any location in the cross-section at the same average velocity.
- Similarly the thermal conductivity at a high shear rate is greater for the lower concentrations than the higher concentrations in cylindrical Couette flow as experimentally shown previously.
- The order of magnitude of increase of the thermal conductivity at the wall is 20 % larger than that of the heat transfer coefficient when Figs. 10 and 14 are compared (approximately an order of 60 % and 40 % increase of thermal conductivity and heat transfer coefficient, respectively).

Finally, the shear-rate-dependent thermal conductivity, as discussed above, affects significantly the heat transfer with a similar order of increase as the heat transfer coefficient.

CONCLUSIONS

Thermal conductivity measurements were made for non-Newtonian fluids in a shear field. A non-Newtonian fluid was used as test fluid, CMC, a purely viscous time-independent fluid.

It was found experimentally that the thermal conductivity increased with shear rate for CMC ($100 \leq \dot{\gamma} \leq 900\ s^{-1}$) solutions with an order of 20-70 % depending on temperature (20-50 °C). The increase of the thermal conductivity with a shear rate was greater for lower concentration solutions than for higher concentration solutions with a difference of 15-30 % for CMC solutions.

As far as the effect of temperature on the thermal conductivity vs. shear rate is concerned in particular, the thermal conductivity of CMC solutions increased with temperature and shear rate. In order to investigate the effect of the shear rate dependence of thermal conductivity on convective heat transfer, a simple parallel plate model with temperature-independent properties was considered. The heat transfer increase was on the order of 30-80 % over the entire temperature range (20-50 °C) of the CMC solutions using the shear-rate-dependent thermal conductivity.

ACKNOWLEDGMENTS

The present research has been supported by the Research Grant of Catholic University of Taegu-Hyosung. The support is greatly appreciated.

NOMENCLATURE

a : half duct width [m]
C_p : specific heat [J/kgK]
f : Darcy friction factor, $\frac{2\frac{dp}{dx}a}{\rho\bar{u}^2}$ [-]
h : convective heat transfer coefficient [W/m^{2}K]
K : power-law fluid consistency [Ns^n/m^2]
k : thermal conductivity for test fluid, k=k($\dot{\gamma}$) [W/mK]
k_0 : zero shear rate thermal conductivity [W/mK]
k_γ : shear-rate-dependent thermal conductivity [W/mK]
$k_{\gamma_{max}}$: thermal conductivity at maximum shear rate [W/mK]
$k_{\gamma_{min}}$: thermal conductivity at minimum shear rate [W/mK]
k^+ : dimensionless thermal conductivity, k_γ/k_0 [-]

l : length of the cylinder [m]
n : power-law flow index [-]
Nu : average Nusselt number for a duct at varying shear rate, ha/k_0
Nu_0 : average Nusselt number for a duct with shear rate independent thermal conductivity, h_0a/k_0 [-]
Pr : Prandtl number, $\eta C_p/k_0$ [-]
Q : total heat transfer [W]
Q_{actual} : actual heat transfer, $Q - Q_{loss}$ [W]
q : total heat flux W/m^2
r : radius [m]
r_i : radius of outer cylinder [m]
r_o : radius of outer cylinder [m]
Re_g : generalized Reynolds number, $\rho\bar{u}^{2-n}a^n/K$ [-]
T : temperature [K or °C]
T_B : bulk temperature of the duct [K or °C]
T_i : temperature of the inner cylinder [K or °C]
T_o : temperature of the outer cylinder [K or °C]
T_w : wall temperature of the plate
U_t : terminal velocity of the falling needle [m/s]
u : velocity in flow direction [m/s]
$\bar{u}$: average velocity in flow direction [m/s]
u_θ : circumferential velocity [m/s]
$\bar{u}^+$: dimensionless average velocity at the varying average velocity [-]
$\bar{u}_0^+$: dimensionless average velocity at the minimum average velocity ($@\bar{u}=\bar{u}_0$) [-]
w_o : angular velocity of the outer cylinder [rad/s]
wppm : parts per million by weight [-]
x : coordinate in flow direction [m]
y : coordinate in transverse direction [m]

Greek Letters

α : inclination angle of shear rate [°]
$\dot{\gamma}$: shear rate [1/s]
$\dot{\gamma}_0$: minimum operating shear rate [1/s]
η_0 : zero shear rate viscosity [$N \cdot s/m^2$]
η_a : apparent viscosity, $\tau/\dot{\gamma}$ [$N \cdot s/m^2$]
μ : dynamic viscosity [$N \cdot s/m^2$]
ν : kinematic viscosity, μ/ρ [m^2/s]
ρ : density of the present test fluid [kg/m^3]
ρ_l : density of the fluid [kg/m^3]
ρ_s : density of the falling needle [kg/m^3]
τ : shear stress [N/m^2]
$\triangle$: difference of quantity [-]
$\triangle T$: temperature difference between inner and outer cylinder wall [K or °C]
$\triangle\bar{u}^+$: difference of dimensionless average velocity, $\bar{u}^+ - \bar{u}_0^+$ [-]

Subscripts

0 : refers to the static condition
$\dot{\gamma}$: refers to the varying shear rate
w : refers to the wall

Superscripts

+ : refers to dimensionless quantities
++ : refers to dimensionless quantities
' : refers to derivative

REFERENCES

Bird, R. B., Armstrong, R. C. and Hassager, O., "Dynamics of Polymeric Liquids", Vol. 1, Wiley, New York, 1977.

Chaliche, M., Delaunay, D. and Bardon, J. P., "Transfort de Chaleur Dans une Configuration Cone-Plateau et Mesure de la Conductivite Thermique en Presence d'une Vitesse de Cisaillement", *Int. J. Heat and Mass Transfer,* **37**, 2381 (1994).

Chitrangad, B. and Picot, J. J. C., "Similarity in Orientation Effects on Thermal Conductivity and Flow Birefringence for Polymers-Polydimethylsiloxane", *Polym. Eng. Sci.,* **21**, 782 (1981).

Cocci, A. A. and Picot, J. J. C., "Rate of Strain Effect on the Thermal Conductivity of a Polymer Liquid", *Polym. Eng. Sci.,* **13**, 337 (1973).

Eckert, E. R. G. and Drake, R. Jr., "Analysis of Heat and Mass Transfer", McGraw-Hill, New York, p. 541 (1972).

Haar, L., Gallagher J. S. and Kell, G. S., "NBS/NRC Steam Tables: Thermodynamic and Transport Properties and Computer Programs for Vapor and Liquid States of Water in SI Units", McGraw-Hill, New York, 1984.

Irvine, T. F. Jr. and Karni, J., "Handbook of Single Phase Convection Heat Transfer, in S. Kakac, R. K. Shah and W. Aung (ed.), Non-Newtonian Fluid Flow and Heat Transfer", chap. 20, Wiley, New York, 1987.

Larson, R. G., "Taylor-Couette Stability Analysis for a Doi-Edwards Fluid", *Rheol. Acta,* **28**, 504 (1989).

Lee, D. L., "Thermal Conductivity Measurements of Non-Newtonian Fluids in a Shear Field", Ph.D. Thesis (Dissertation Adviser: Thomas F. Irvine, Jr.), Mech. Eng. Dept., State Univ. of New York at Stony Brook, 1995.

Loulou, T., Peerhossaini, H. and Bardon, J. P., "Etude Experimentale de la Conductivite Thermique de fluides Non-Newtoniens sous Cisaillement Application Aux Solutions de Carbopol 940", *Int. J. Heat and Mass Transfer,* **35**, 2557 (1992).

Park, N. A., "Measurement of Rheological Properties of Non-Newtonian Fluids with Falling Needle Viscometer", Ph. D. Thesis, Mech. Eng. Dept., State Univ. of New York, Stony Brook, 1984.

Park, N. A., Cho, Y. I. and Irvine, T. F. Jr., "Steady Shear Viscosity Measurements of Viscoelastic Fluids with the Falling Needle Viscometer", *J. of Non-Newtonian Fluid Mechanics,* **34**, 351 (1990).

Park, N. A. and Irvine, T. F. Jr., "Measurements of Rheological Fluid Properties with the Falling Needle Viscometer", *Rev. Sci. Insts.,* **59**, 9 (1988).

Sinevic, V., Kuboi, R. and Nienow, A. W., "Power Numbers, Taylor Numbers and Taylor Vortices in Viscous Newtonian and Non-Newtonian Fluids", *Chem. Eng. Sci.,* **41**, 2915 (1986).

Taylor, G. I., "Stability of a Viscous Fluid Contained between Two Concentric Rotating Cylinders", *Phil. Trans.,* **A223**, 289 (1923).

Wallace, D. J., Moreland, C. and Picot, J. J. C., "Shear Dependence of Thermal Conductivity in Polyethylene Melts", *Polym. Eng. Sci.,* **25**, 70 (1985).